NATIONAL ADVISORY COMMITTEE FOR AERONAUTICS

TECHNICAL NOTE 4401

HYDRODYNAMIC IMPACT LOADS ON 30° AND 60° V-STEP PLAN-FORM MODELS WITH AND WITHOUT DEAD RISE

By Philip M. Edge, Jr., and Jean P. Mason

Langley Aeronautical Laboratory
Langley Field, Va.

Washington
September 1958

NATIONAL ADVISORY COMMITTEE FOR AERONAUTICS

TECHNICAL NOTE 4401

HYDRODYNAMIC IMPACT LOADS ON 30° AND 60° V-STEP PLAN-FORM MODELS WITH AND WITHOUT DEAD RISE

By Philip M. Edge, Jr., and Jean P. Mason

SUMMARY

Hydrodynamic impact loads of 30° and 60° included-angle V-step models were investigated at the Langley impact basin. The investigation consisted of a series of fixed-trim impacts in smooth water with a dead-rise model having a round keel and chine flare and a beam-loading coefficient of 3.6. Impact loads and motions for a range of trim and flight-path angles were measured to determine effects of step plan-form angle and for comparison with data for a flat-bottom model.

The data are presented in a table, and typical time histories and variations of maximum impact lift and maximum draft with trim and flight-path angle are included. Over the range of the tests the maximum loads for the 30° V-step model are shown to be as much as 29 percent less than those for the 60° V-step model. Effects of dead rise for the 30° V-step model are shown to indicate that this configuration experiences loads as small as 50 percent of those experienced by a similar V-step flat-bottom model.

INTRODUCTION

Hydrodynamic impact loads have been studied to determine effects of basic model configurations on impact loads. The data obtained from these studies have established fundamental relationships of transverse shape, longitudinal shape, and step plan-form shape with hydrodynamic impact loads (refs. 1 to 9). However, step plan-form investigations of this type have been concerned only with a flat-bottom model of 28° V-step (data reported in ref. 8 and compared with data of a transverse-step model in ref. 9). Modern seaplanes generally are designed with hulls or hydro-skis having dead rise and step or stern plan forms of larger included angles. The purpose of the present investigation was to obtain data as to the effects of plan-form angle and dead rise on impact loads.

A series of fixed-trim impacts were made in the Langley impact basin with dead-rise models of 30° and 60° included plan-form angles at the

stern. The transverse shape of these models consisted of a round bottom at the keel and chine flare with an intermediate straight section. The models had a beam-loading coefficient of 3.6 and were designed to represent the forebody portion of a V-step hull; however, they can also be considered as representative of lightly loaded hydro-skis. Impacts were made in smooth water over a range of trim and initial flight-path angles, and the resulting impact loads, moments, and motions were recorded throughout each impact.

This paper presents the data obtained in the impacts and shows variations of maximum loads and drafts with trim and flight-path angles. Comparisons are made of the data for the 30° and 60° plan-form angles to indicate the effects of plan-form angle, and the data for the 30° plan-form angle are compared with the flat-bottom data of reference 8 to show dead-rise effects for the V-step plan form.

SYMBOLS

b	model beam, ft
C_d	draft coefficient, $\frac{z}{b}$
C_L	impact lift coefficient, $\frac{n_i W}{\frac{1}{2}\rho V_o^2 b^2} = \frac{F_v}{\frac{1}{2}\rho V_o^2 b^2}$
C_m	pitching-moment coefficient, $\frac{M_Y}{\frac{1}{2}\rho V_o^2 b^3}$
C_t	time coefficient, $\frac{V_o t}{b}$
$C_{\dot{z}}$	vertical-velocity coefficient, $\frac{\dot{z}}{\dot{z}_o}$
C_Δ	beam-loading coefficient, $\frac{W}{\rho g b^3}$
F_n	hydrodynamic force normal to keel, lb
F_v	vertical component of hydrodynamic force, lb

g	acceleration due to gravity, 32.2 ft/sec^2
M_Y	pitching moment about step, lb-ft
n_i	impact load factor normal to undisturbed water surface, $\frac{F_V}{W}$
t	time after contact, sec
V	resultant velocity of model, fps
W	dropping weight, lb
$\dot{x}$	velocity of model parallel to undisturbed water surface, fps
z	draft of model normal to undisturbed water surface, ft
$\dot{z}$	velocity of model normal to undisturbed water surface, fps
γ	flight-path angle relative to undisturbed water surface, deg
ρ	mass density of water, 1.938 slugs/cu ft
τ	trim angle, deg

Subscripts:

o	instant of initial contact with water surface
max	maximum

APPARATUS

Tests were made in the Langley impact basin with the equipment described in reference 10. This equipment consists of a catapult, an arresting gear, instrumentation for measuring loads and motions of the model, and a testing carriage to which the model is attached at all times by a boom. The boom is mounted on a parallel linkage which permits the model to move freely in the vertical direction while the carriage is moving horizontally down the tank.

Model

The model tested had a V-shape plan form at each end with a 5-foot section of constant beam (22 inches) in the center. (See fig. 1.) At

one end the included angle of the V plan form was 30° and at the other end, 60°. The model, which was of wood covered with fiber glass, was constructed so that it could be mounted to its attachment fitting with either end as the stern (or step). Figure 2 shows the model mounted on the carriage boom as a 30° V-step plan-form model and as a 60° V-step plan-form model. This mounting held the model fixed in trim throughout the impacts.

The transverse shape of the model, as shown in figure 1, was round at the keel with a straight midsection of about 35° dead-rise angle and with chines flared to the horizontal. At the ends of the model the outboard portions of this cross section were cut away to form the V plan form.

Instrumentation

The instrumentation consisted of a multichannel oscillograph, accelerometers, a dynamometer, water-contact indicator, and electrical circuits for measuring displacements and velocities. All measurements were recorded on the oscillograph along with 0.01-second timing.

Accelerations in the vertical direction were measured by oil-damped unbonded strain-gage-type accelerometers whose frequency responses were flat to above 60 cycles per second. Loads normal to the keel of the model and pitching moments about the stern were obtained from a strain-gage-type dynamometer mounted between the model and the carriage boom and from consideration of the inertia effects of the mass below the dynamometer.

Initial contact of the model with the water and rebound from the water were determined from a pulse produced by an electrical circuit which was completed by the water through contacts in the model. Horizontal velocity was computed from photo-electric-cell indications of horizontal displacement and from the recorded time. Vertical displacement was obtained from a slidewire and vertical velocity was obtained from electrical differentiation of the slidewire displacement.

In general, the data obtained are believed to be accurate within the following limits:

Horizontal velocity, ft/sec	±0.5
Vertical velocity, ft/sec	±0.2
Vertical displacement, ft	±0.02
Acceleration, g units	±0.2
Weight, lb	±10
Time, sec	±0.002
Pitching moment, percent	±5

TEST PROCEDURE

This investigation consisted of a series of forward-speed impacts in smooth water with each model at trim angles of 4°, 8°, 16°, and 30° over a range of initial flight-path angles from 3° to 20°. Impacts without forward speed $\left(\gamma_o = 90^\circ\right)$ were made at $\tau = 0^\circ$ and with each model at $\tau = 8^\circ$ over a range of vertical velocities $\left(\dot{z}_o = 3 \text{ to } 10 \text{ fps}\right)$. All impacts were made at a beam-loading coefficient of 3.6 (W = 1,375 pounds). Throughout the immersion a lift force equal to the total weight of the model was applied to simulate a wing lift of 1 g, as described in reference 10.

RESULTS AND DISCUSSION

The experimental data obtained in this investigation are presented in table I for each of the impacts made. This table shows the measured values of loads and motions at contact with the water, at maximum acceleration, at maximum pitching moment, at maximum draft, and at rebound.

Sample time histories of typical variations of the data obtained throughout the impacts are presented in figure 3 for impacts without forward speed and in figure 4 for impacts with forward speed. In figure 3, data are shown for impacts at 0° and 8° trim. From figure 3(a) it is seen that the loads at 0° trim build up rather rapidly with the full-length contact of the flat portion of the round keel. As immersion continues the peak load is attained on the rounded portion of the cross section and a reduction in load is experienced during immersion of the straight portion of the cross section where the bottom slope is approximately 35°. A second sharp increase in load is encountered as the low angle of the flared chines becomes involved. This characteristic of the load application can to some extent be expected throughout the impacts of a model having a similar cross section. However, with increased trim (fig. 3(b)) and forward speed (fig. 4), the geometry of the immersed portion of the model can be expected to be such that the loads are less rapidly applied and the effects of the chine flare on the impact loads are small or nonexistent. From figure 3(b) and figure 4, comparisons of the time histories for the two models show that the loads are applied similarly for the 30° and 60° V-step plan-form configuration. This comparison shows that the loads build up earlier during the impact of the 60° V-step, the model being slowed more rapidly with less draft and pitching moment than is experienced by the 30° V-step model.

In figures 5 and 6 the variations of maximum impact lift and maximum draft coefficients with initial flight-path angle for the 30° and

60° V-step plan-form models at 8° and 30° trim are compared. From the comparisons of the maximum draft coefficients, it is seen that the effect of step plan-form angle is more evident at the higher trim of 30°, and the maximum draft of the 60° V-step model is 20 percent less than that of the 30° V-step plan-form model.

The relations of the maximum impact lift coefficient and trim angle for the two V-step plan-form configurations are further illustrated in figures 7 and 8. Figure 7 shows the variation of the maximum impact lift coefficient with trim angle for the two models at four initial flight-path angles. The curves of this figure were obtained from faired curves of $C_{L,max}$ plotted against γ_o for each trim. (For example, see fig. 5.) Figure 8 shows the variation of the ratio of the maximum loads for the two models (from fig. 7) with trim angle. From the comparison shown in figures 7 and 8, it is seen that at low trim angles (4°) the loads for the 30° V-step model are within 10 percent of those for the 60° V-step model. The greatest difference in load occurs with the combination of high trim and low initial flight-path angles where the load of the 30° V-step model is 29 percent less than the load of the 60° V-step model.

Effects of dead rise on maximum loads for V-step plan-form configurations can be estimated by comparing the data of the present investigation for the dead-rise model with the data of reference 8 for a V-step flat-bottom model. The data of reference 8 were obtained under conditions similar to those of the present test and are for a V-step model having an included plan-form angle of 28° and a beam-loading coefficient of 4.6. These data are corrected to a beam-loading coefficient of 3.6 by applying an 8-percent correction based on maximum lift coefficient inversely proportional to $(C_\Delta)^{1/3}$ (ref. 11). The corrected data are compared with the 30° V-step data of the present investigation in figure 9. This figure shows the variations of the ratio of the maximum impact lift coefficient for the dead-rise model to that for the flat-bottom model with angle of trim. This comparison indicates that this dead-rise configuration experiences maximum impact lift coefficients which are 25 percent less than the maximum impact lift coefficients of the flat-bottom model at 20° trim and 50 percent less at 4° trim.

CONCLUSIONS

An investigation of the impact loads on models of 30° and 60° V-step plan form and having a flat bottom or a rounded cross section near the keel results in the following conclusions:

1. The maximum loads for the 30° V-step model at low trims (4°) are within 10 percent of those for the 60° V-step model. At landing conditions of high trims and low flight-path angles, the maximum loads for the 30° V-step model are 29 percent less than those for the 60° V-step model.

2. The dead-rise configuration experienced maximum loads which are 25 percent less than those of the flat-bottom model at 20° trim and 50 percent less at 4° trim.

Langley Aeronautical Laboratory,
National Advisory Committee for Aeronautics,
Langley Field, Va., July 24, 1958.

REFERENCES

1. Edge, Philip M., Jr.: Hydrodynamic Impact Loads in Smooth Water for a Prismatic Float Having an Angle of Dead Rise of 10°. NACA TN 3608, 1956.

2. McArver, A. Ethelda: Water-Landing Investigation of a Model Having Heavy Beam Loadings and 0° Angle of Dead Rise. NACA TN 2330, 1951.

3. Batterson, Sidney A., and McArver, A. Ethelda: Water Landing Investigation of a Model Having a Heavy Beam Loading and a 30° Angle of Dead Rise. NACA TN 2015, 1950.

4. Edge, Philip M., Jr.: Impact-Loads Investigation of Chine-Immersed Models Having Concave-Convex Transverse Shape and Straight or Curved Keel Lines. NACA TN 3940, 1957.

5. Edge, Philip M., Jr.: Impact-Loads Investigation of Chine-Immersed Model Having a Circular-Arc Transverse Shape. NACA TN 4103, 1957.

6. Edge, Philip M., Jr., and Mixson, John S.: Impact-Loads Investigation of a Chine-Immersed Model Having a Longitudinally Curved Bow and a V-Bottom With a Dead-Rise Angle of 30°. NACA TN 4106, 1957.

7. Edge, Philip M., Jr.: Hydrodynamic Impact Loads of a -20° Dead-Rise Inverted-V Model and Comparisons With Loads of a Flat-Bottom Model. NACA TN 4339, 1958.

8. Miller, Robert W.: Water-Landing Investigation of a Flat-Bottom V-Step Model and Comparison With a Theory Incorporating Planing Data. NACA TN 2932, 1953.

9. Miller, Robert W.: Comparison of Experimental Hydrodynamic Impact Loads and Motions for a V-Step and a Transverse-Step Hydro-Ski. NACA RM L53K20a, 1954.

10. Batterson, Sidney A.: The NACA Impact Basin and Water Landing Tests of a Float Model at Various Velocities and Weights. NACA Rep. 795, 1944. (Supersedes NACA WR L-163.)

11. Schnitzer, Emanuel: Reduction of Hydrodynamic Impact Loads for Waterborne Aircraft. NACA RM L55E09b, 1955.

TABLE I.- IMPACT-LOADS DATA FROM TESTS OF V-STEP PLAN-FORM MODELS

[C_Δ = 3.6; W = 1,375 lb]

Impact	Trim, τ, deg	At contact			At $n_{i,max}$							At $M_{Y,max}$			At z_{max}			At rebound	
		$\dot{z}_o$, fps	$\dot{x}_o$, fps	γ_o, deg	t, sec	n_i	F_n, lb	z, ft	$\dot{z}$, fps	M_Y, lb-ft	C_L	t, sec	M_Y, lb-ft	n_i	t, sec	n_i	z, ft	t, sec	$\dot{z}$, fps
30° V-step model																			
1		3.56			0.213	0.23	312	0.707	2.71	1,524	7.60	0.238	1,623	0.23	0.583	0.18	1.157	———	———
2		4.65			.153	.38	497	.666	3.66	2,351	7.44	.188	2,704	.35	.553	.22	1.294	———	———
3		5.48			.135	.47	631	.690	4.34	3,199	6.61	.157	3,418	.46	.547	.22	1.597	———	———
4		6.78	0	90	.097	.69	915	.625	5.81	4,106	6.29	.139	4,942	.60	.534	.25	1.684	———	———
5	4	8.57			.082	1.13	1473	.651	7.30	6,783	6.48	.110	8,549	.96	.533	.25	1.963	———	———
6		9.93			.083	1.54	2166	.779	8.27	11,696	6.58	.088	12,204	1.53	.543	.30	2.246	———	———
7		11.08			.075	1.83	2509	.726	9.38	11,998	6.28	.083	13,867	1.80	.548	.28	2.456	———	———
8		4.62			.257	.27	381	1.380	2.50	1,662	5.40	.323	1,816	.27	.672	.18	1.729	———	———
9		5.47			.219	.35	492	1.097	4.12	2,202	4.95	.264	2,409	.24	.649	.20	1.863	———	———
10		6.71	0	90	.155	.51	713	.993	5.55	2,956	4.75	.200	3,303	.46	.625	.22	2.096	———	———
11	8	8.56			.116	.69	962	1.079	6.29	4,388	3.99	.197	5,084	.57	.617	.18	2.274	———	———
12		9.26			.119	.92	1274	1.058	7.55	5,855	4.54	.173	6,495	.73	.606	.22	2.587	———	———
13		11.01			.090	1.30	1830	.958	9.43	7,737	4.52	.137	9,312	1.07	.607	.21	2.781	———	———
14		4.27	91.74	2.60	.123	.98	1353	.416	2.35	5,442	.05	.130	5,580	.97	.195	.75	.491	0.556	-1.46
15		6.10	78.13	4.46	.110	1.49	2092	.562	3.57	9,552	.10	.116	9,736	1.44	.190	.82	.676	.580	-1.78
16		8.19	66.67	7.00	.084	2.10	2969	.618	5.72	13,286	.20	.104	14,575	1.82	.206	.65	.846	.586	-1.72
17	4	10.22	53.76	10.76	.069	2.63	3780	.650	7.92	17,105	.37	.090	18,904	2.18	.295	.28	1.140	1.103	-1.17
18		10.59	42.02	14.15	.064	2.60	3661	.641	8.72	5,411	.58	.084	19,048	2.18	.379	.24	1.373	———	———
19		8.99	22.94	21.40	.079	1.58	2235	.662	7.13	10,943	1.10	.098	12,122	1.38	.484	.23	1.580	———	———
20		4.55	78.13	3.33	.161	.95	1399	.573	1.97	3,909	.07	.176	4,244	.93	.226	.73	.620	.469	-2.04
21		6.15	74.07	4.75	.159	1.45	2093	.741	2.33	7,443	.11	.159	7,443	1.15	.209	1.11	.777	.541	-2.45
22		8.31	68.26	6.94	.119	2.22	3101	.816	4.55	12,345	.20	.119	12,345	2.22	.184	1.36	.934	.521	-3.17
23		9.20	54.79	9.53	.104	2.02	3047	.850	6.13	12,063	.28	.112	12,496	1.98	.214	.86	1.104	.660	-2.68
24		9.14	47.39	10.92	.103	1.70	2581	.838	6.39	10,203	.31	.113	10,688	1.66	.240	.72	1.182	.792	-1.91
25	8	11.17	56.82	11.12	.086	2.74	4033	.848	7.75	15,999	.35	.100	16,973	2.61	.198	1.06	1.170	.630	-3.07
26		11.24	53.76	11.81	.090	2.68	3932	.881	7.50	15,579	.38	.105	16,638	2.50	.207	.99	1.227	.689	-2.64
27		11.19	43.96	14.28	.090	2.42	3507	.907	7.97	14,144	.50	.105	15,375	2.25	.243	.68	1.339	.846	-2.09
28		9.25	28.25	18.13	.110	1.42	2066	.934	6.76	8,973	.68	.149	9,507	1.16	.340	.34	1.468	———	———
29		9.34	19.38	25.73	.118	1.26	1802	1.008	6.94	8,334	1.15	.142	9,616	1.27	.169	.23	1.796	———	———
30		4.36	89.29	2.80	.204	1.04	1478	.589	.82	2,671	.06	.218	2,831	.98	.223	.95	.594	.512	-2.55
31		5.92	78.43	4.32	.177	1.38	2021	.758	1.75	4,365	.09	.187	4,523	1.34	.207	1.26	.777	.471	-3.94
32		8.87	66.67	7.58	.156	2.01	2986	1.049	3.20	6,304	.19	.178	8,693	1.92	.196	1.78	1.096	.486	———
33	16	8.90	54.35	9.30	.172	1.78	2722	1.173	3.44	8,400	.25	.196	8,488	1.67	.221	1.38	1.229	.552	-4.44
34		10.31	38.68	14.93	.150	1.76	2669	1.314	6.10	9,149	.46	.160	9,397	1.74	.263	1.04	1.585	.760	-3.57
35		10.57	27.47	21.05	.150	1.44	2178	1.392	7.13	7,786	.70	.165	8,154	1.42	.337	.55	1.894	2.186	-1.70
36		3.33	92.59	2.06	.225	.88	1409	.518	———	2,177	.04	.225	2,177	.88	.238	.85	.518	.514	———
37		4.07	78.74	2.96	.215	1.19	1988	.766	———	3,227	.08	.215	3,227	1.19	.230	1.18	.766	.503	———
38		7.66	66.67	6.55	.204	1.68	2757	1.131	1.81	5,445	.16	.210	5,752	1.66	.227	1.53	1.145	.512	———
39		9.68	53.19	10.31	.195	1.75	2955	1.470	3.63	6,944	.25	.215	7,639	1.74	.245	1.60	1.537	.582	———
40	30	10.49	38.17	15.37	.206	1.61	2714	1.768	———	7,586	.43	.208	7,717	1.58	.287	1.21	1.927	.746	———
41		10.56	27.32	21.13	.213	1.33	2213	1.909	6.08	6,648	.65	.233	6,856	1.26	.361	.70	2.282	1.000	-3.19
60° V-step model																			
42		3.72			.093	.41		.305	2.34		12.63				.506	.14	.858	———	———
43		5.99			.057	.95		.303	4.96		11.16				.504	.18	1.231	———	———
44		7.68	0	90	.048	1.77		.333	6.11		12.70				.531	.19	1.518	———	———
45	0	9.24			.042	2.24		.112	9.11		11.08				.557	.18	1.772	———	———
46		10.88			.037	3.03		.362	9.13		10.82				.536	.23	2.032	———	———
47		3.55			.216	.19	253	.734	2.96	764	6.37	.766	1,296	.06	.741	.11	1.448	———	———
48		5.96			.117	.43	550	.674	5.26	1,586	5.11	.217	2,130	.40	.667	.11	1.818	———	———
49		7.17	0	90	.117	.60	793	.800	6.01	2,552	4.93	.162	3,075	.55	.632	.17	2.021	———	———
50	8	8.22			.094	.75	995	.748	7.33	2,926	4.69	.174	4,359	.62	.619	.19	2.262	———	———
51		9.60			.078	1.00	1384	.728	8.52	3,910	4.58	.148	5,677	.83	.663	.13	2.461	———	———
52		10.75			.076	1.24	1831	.809	9.48	5,782	4.90	.098	7,174	1.25	.638	.15	2.617	———	———
53		4.58	81.30	3.22	.117	1.12	1662	.425	2.32	5,544	.07	.117	5,544	1.12	.192	.56	.470	.555	-0.83
54		6.68	65.36	5.84	.089	1.54	2278	.521	2.26	8,196	.15	.114	8,740	1.33	.219	.40	.715	———	———
55		9.30	52.08	10.12	.066	2.36	3351	———	7.19	12,606	.36	.100	14,428	1.76	.325	———	———	———	———
56	4	10.80	40.98	14.76	.063	2.80	3917	.627	8.41	16,702	.66	.094	16,702	1.99	.363	.27	1.297	———	———
57		9.21	25.13	20.13	.066	1.84	2547	.540	7.63	10,298	1.09	.094	11,091	1.43	.459	.22	1.431	———	———
58		4.52	75.63	3.42	.124	1.09	1623	.436	2.08	3,788	.08	.127	3,872	1.09	.187	.75	.474	.480	-1.53
59		10.62	71.94	8.40	.074	3.44	5066	.691	7.43	14,757	.27	.095	15,762	2.98	.250	1.49	.884	.434	-3.66
60		10.34	60.24	9.74	.075	2.88	4171	.705	7.42	12,104	.33	.100	13,682	2.43	.282	1.02	.953	.539	-2.77
61		10.57	58.82	10.19	.075	2.77	4137	.709	7.76	11,977	.33	.105	13,269	2.30	.277	1.07	.971	.572	-2.51
62	8	9.56	37.88	14.16	.082	2.00	2860	.705	7.36	8,900	.55	.113	9,712	1.65	.253	.53	1.145	.963	- .94
63		10.97	30.30	19.90	.077	2.09	3000	.777	8.75	9,390	.85	.103	10,457	1.74	.328	.33	1.450	———	———
64		10.40	25.51	22.18	.066	1.90	2681	.649	8.97	7,383	1.06	.106	9,649	1.55	.390	.27	1.528	———	———
65		4.40	76.92	3.27	.114	1.03	1680	.463	1.57	2,802	.07	.179	2,988	.94	.179	.93	.479	.439	-1.97
66		10.59	71.43	8.43	.095	3.40	5124	.846	6.11	11,437	.28	.107	11,627	3.24	.149	2.32	.949	.369	-5.04
67		10.32	59.17	9.89	.101	2.90	4358	.868	5.74	10,416	.34	.116	10,638	2.73	.158	1.98	.984	.411	-4.88
68	16	10.45	40.98	14.31	.116	2.08	3138	.966	7.06	7,996	.49	.118	8,379	1.97	.221	1.06	1.262	.664	-2.86
69		10.46	25.77	22.09	.112	1.49	2217	1.035	7.82	5,871	.81	.152	6,571	1.34	.267	.38	1.633	———	———
70		4.18	75.76	3.16	.158	1.11	2092	.490	1.26	2,590	.08	.163	2,885	1.11	.188	1.03	.497	.409	-2.73
71		7.41	70.42	6.01	.131	2.25	3863	.749	2.88	6,455	.19	.145	6,764	2.22	.162	2.02	.773	.360	-5.12
72		10.29	58.48	9.98	.127	2.86	4908	1.038	4.79	9,237	.34	.149	9,773	2.74	.166	2.47	1.103	.392	-6.41
73	30	10.72	40.00	15.00	.152	2.06	3464	1.333	5.64	7,437	.51	.175	7,483	1.95	.235	1.44	1.488	.597	-4.87
74		9.54	23.81	21.83	.167	1.13	1869	1.376	6.38	4,271	.72	.221	4,582	1.04	.391	.43	1.883	———	———

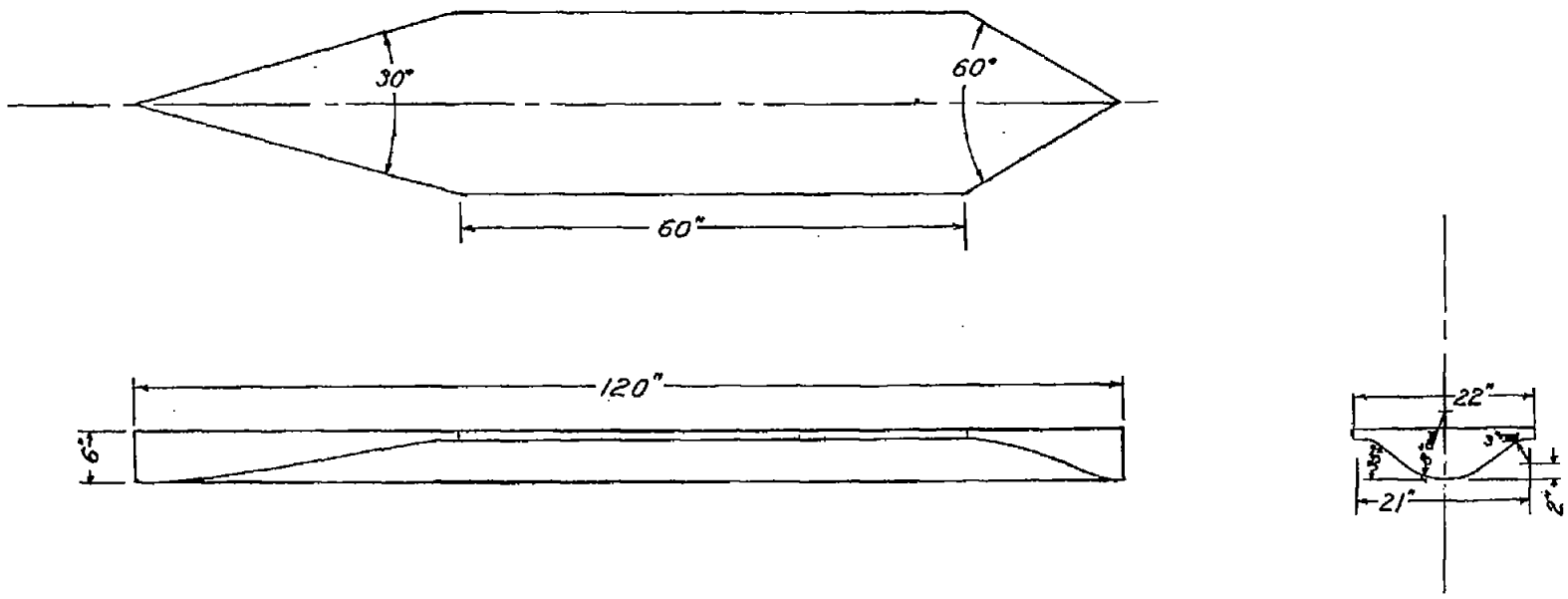

Figure 1.- Drawing of model.

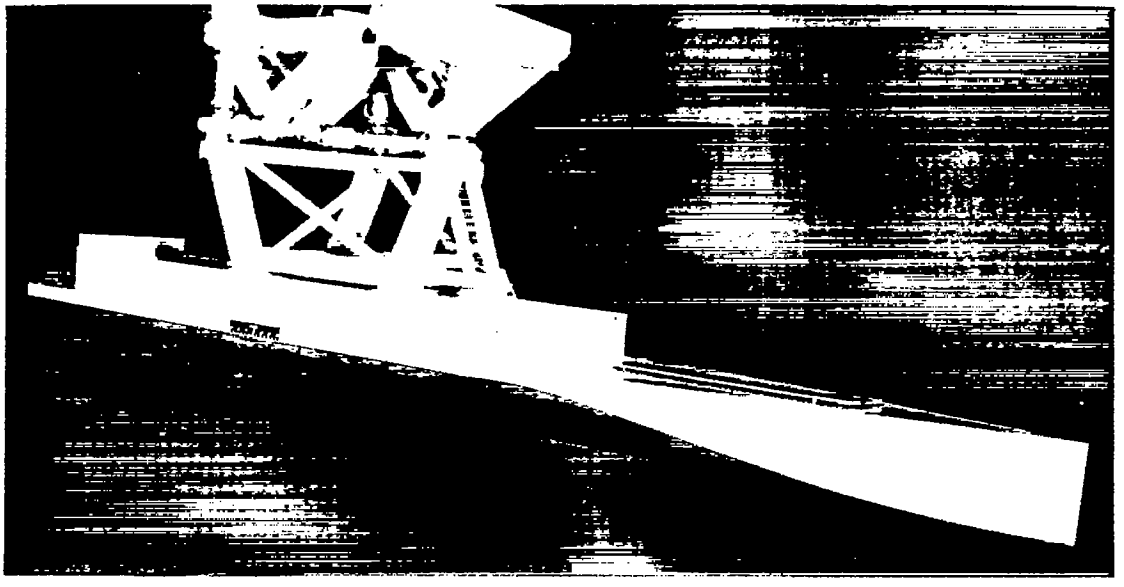

(a) 30° V-step model. L-57-2673

(b) 60° V-step model. L-58-34

Figure 2.- Models on carriage.

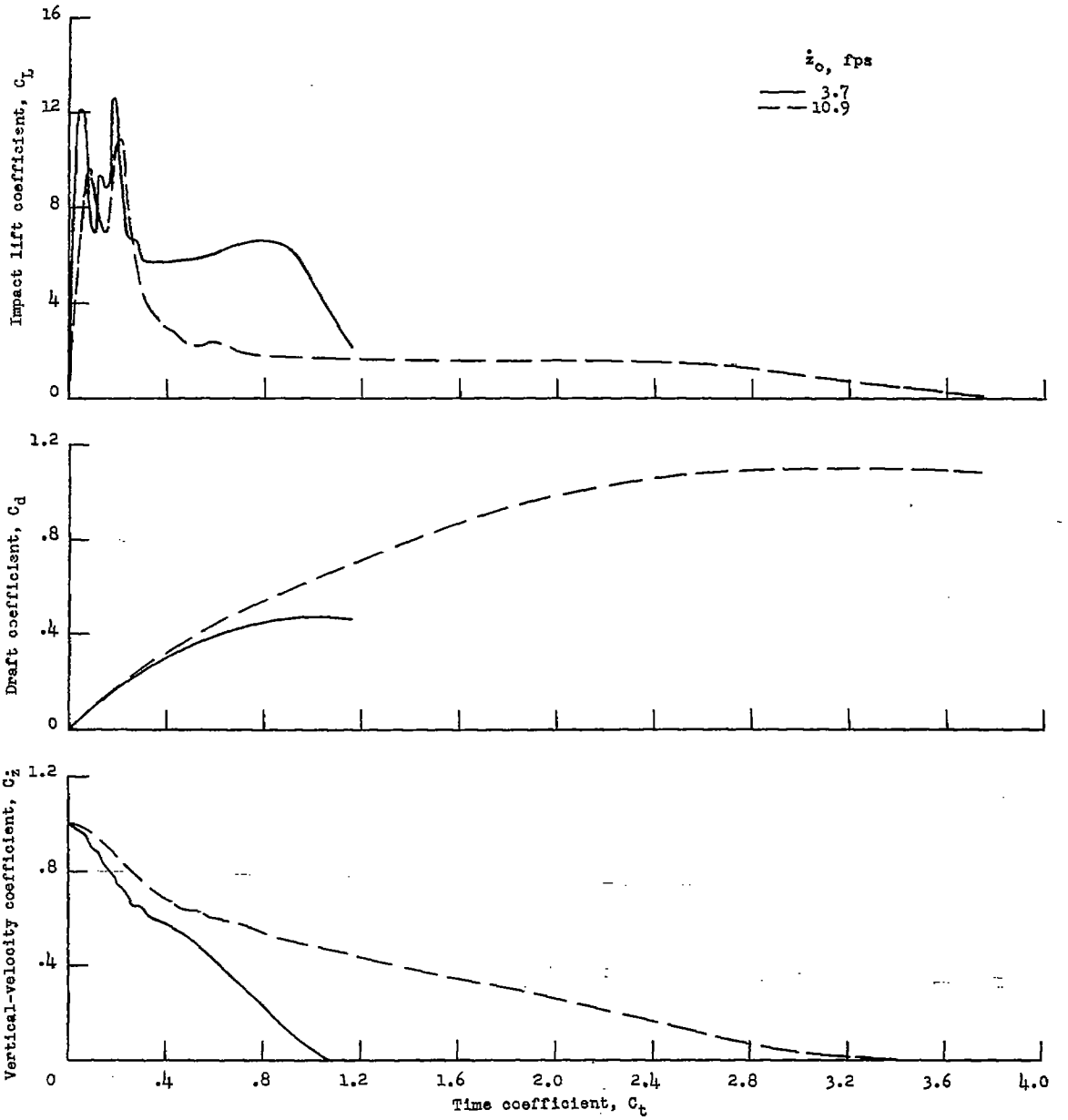

(a) $\tau = 0^\circ$.

Figure 3.- Variations of load and motion coefficients with time coefficient for impacts without forward speed.

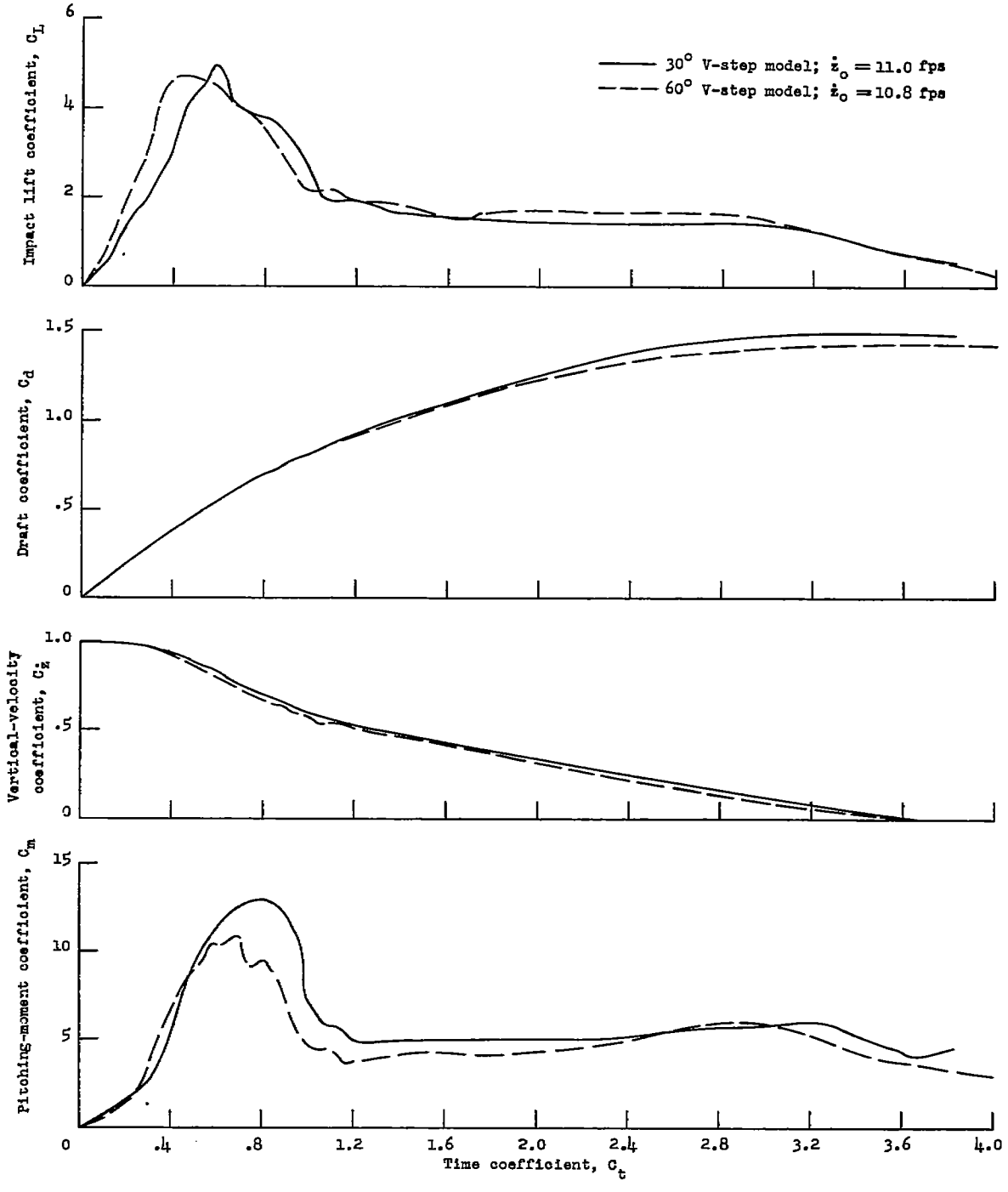

(b) $\tau = 8^\circ$.

Figure 3.- Concluded.

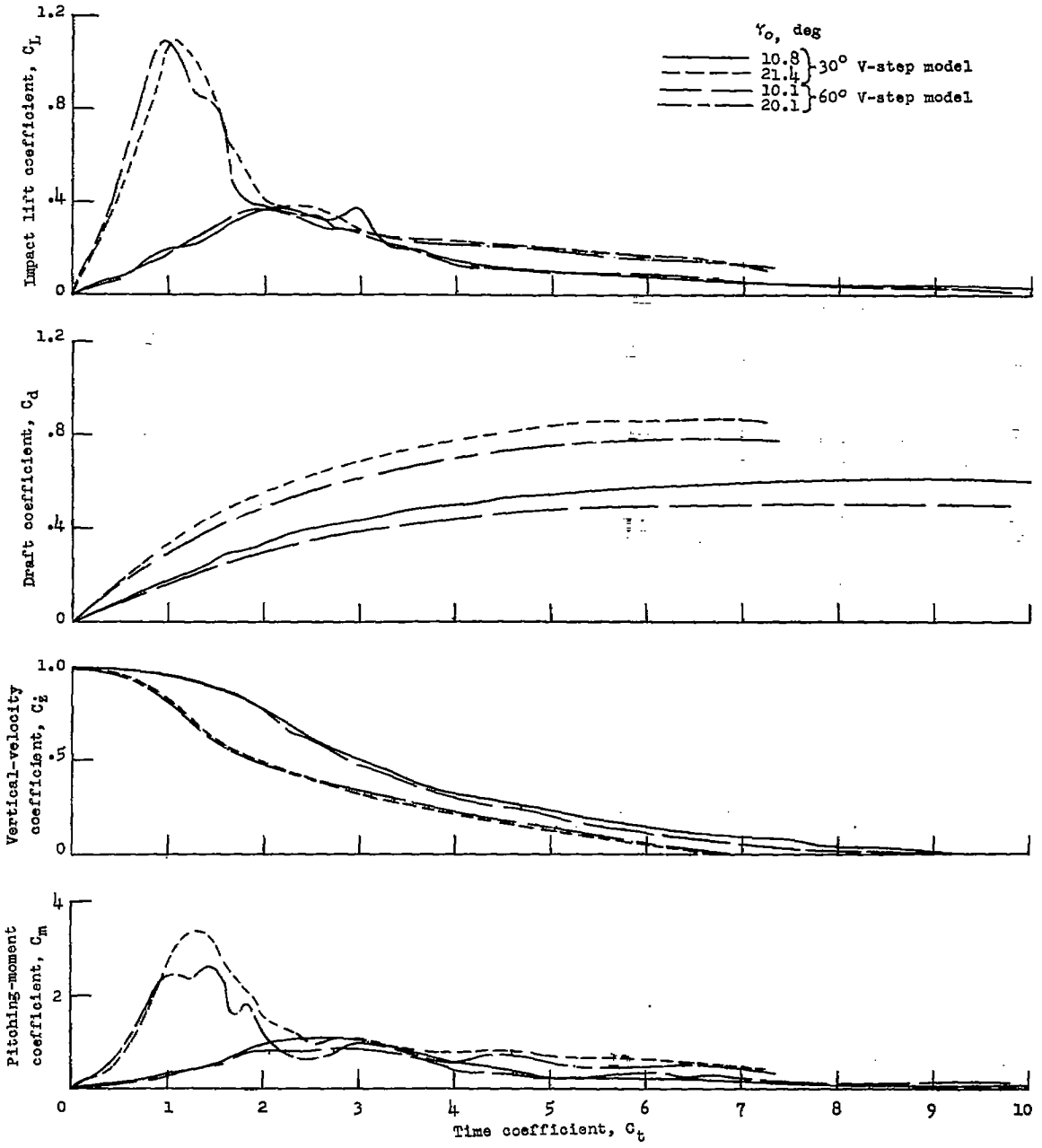

(a) $\tau = 4^\circ$.

Figure 4.- Variations of load and motion coefficients with time coefficient for impacts with forward speed.

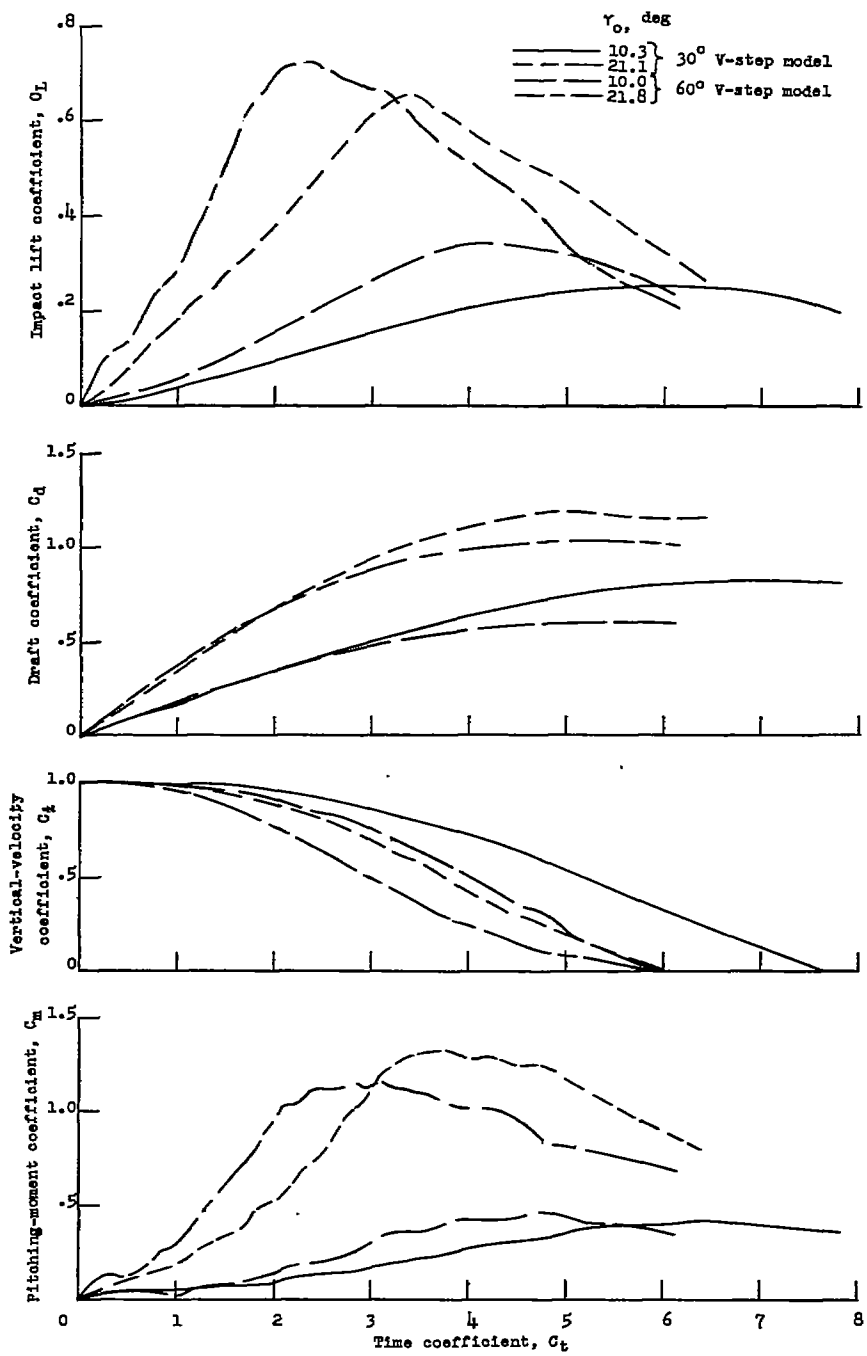

(b) $\tau = 30°$.

Figure 4.- Concluded.

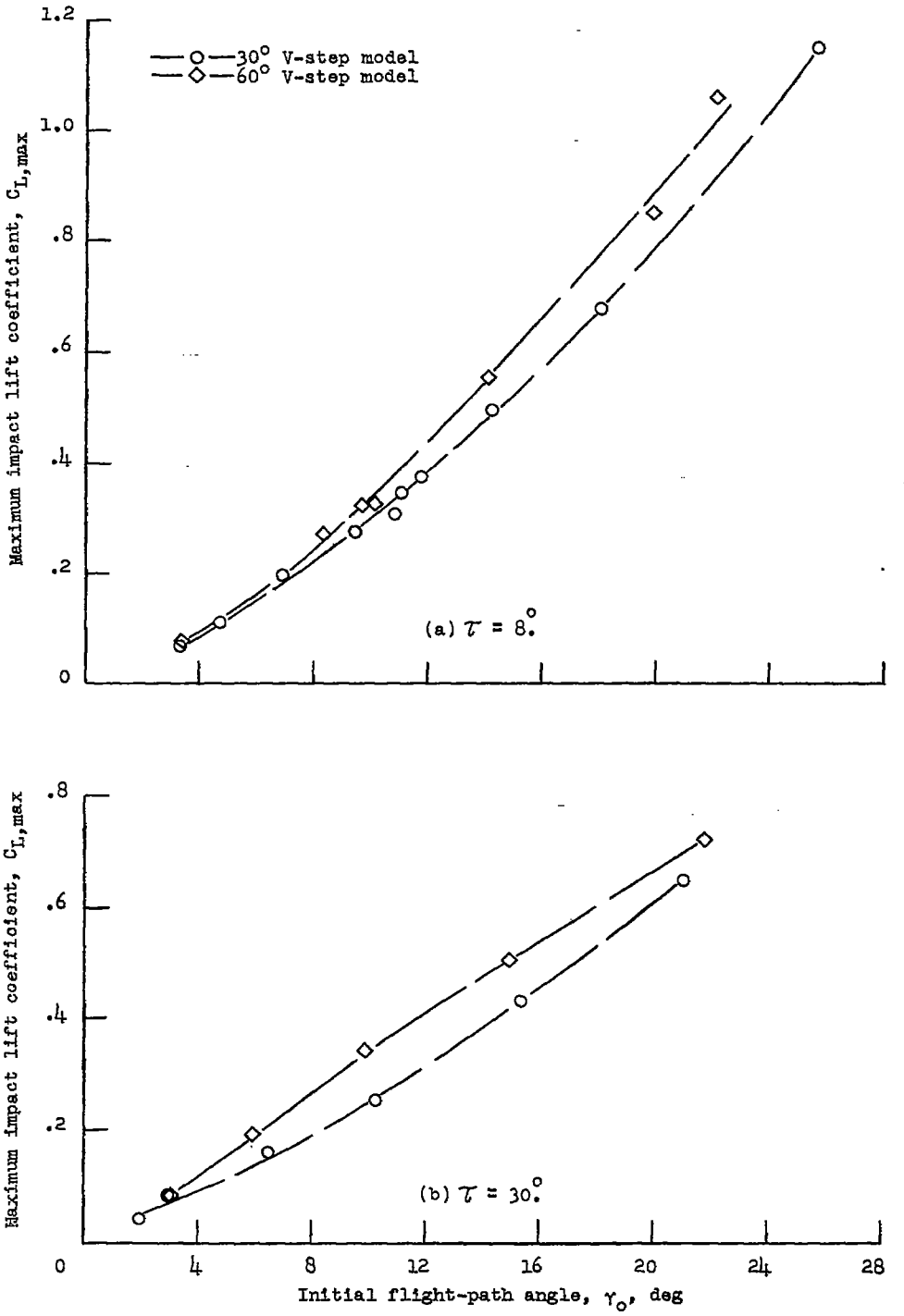

Figure 5.- Variations of impact lift coefficient with initial flight-path angle.

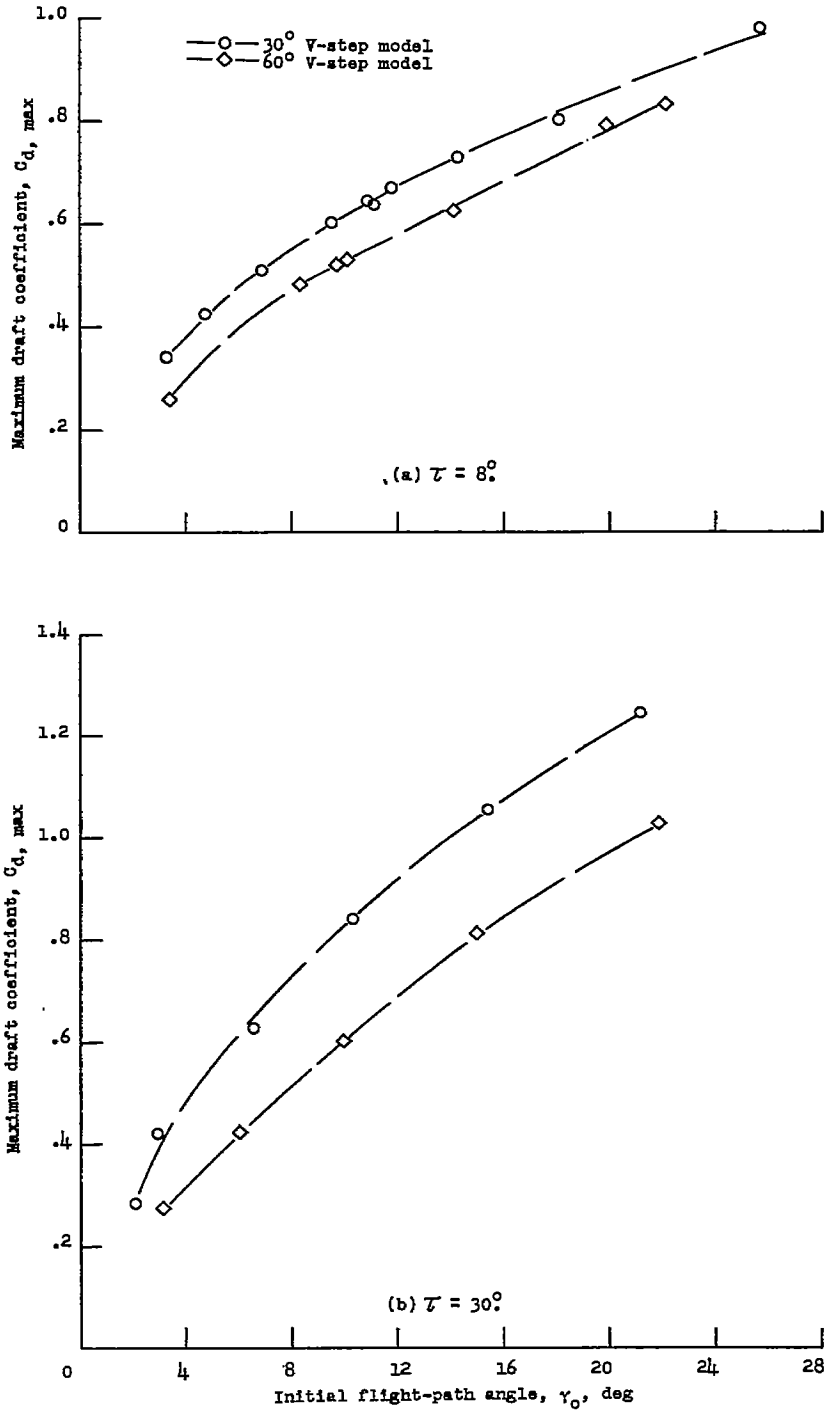

Figure 6.- Variations of draft coefficient with initial flight-path angle.

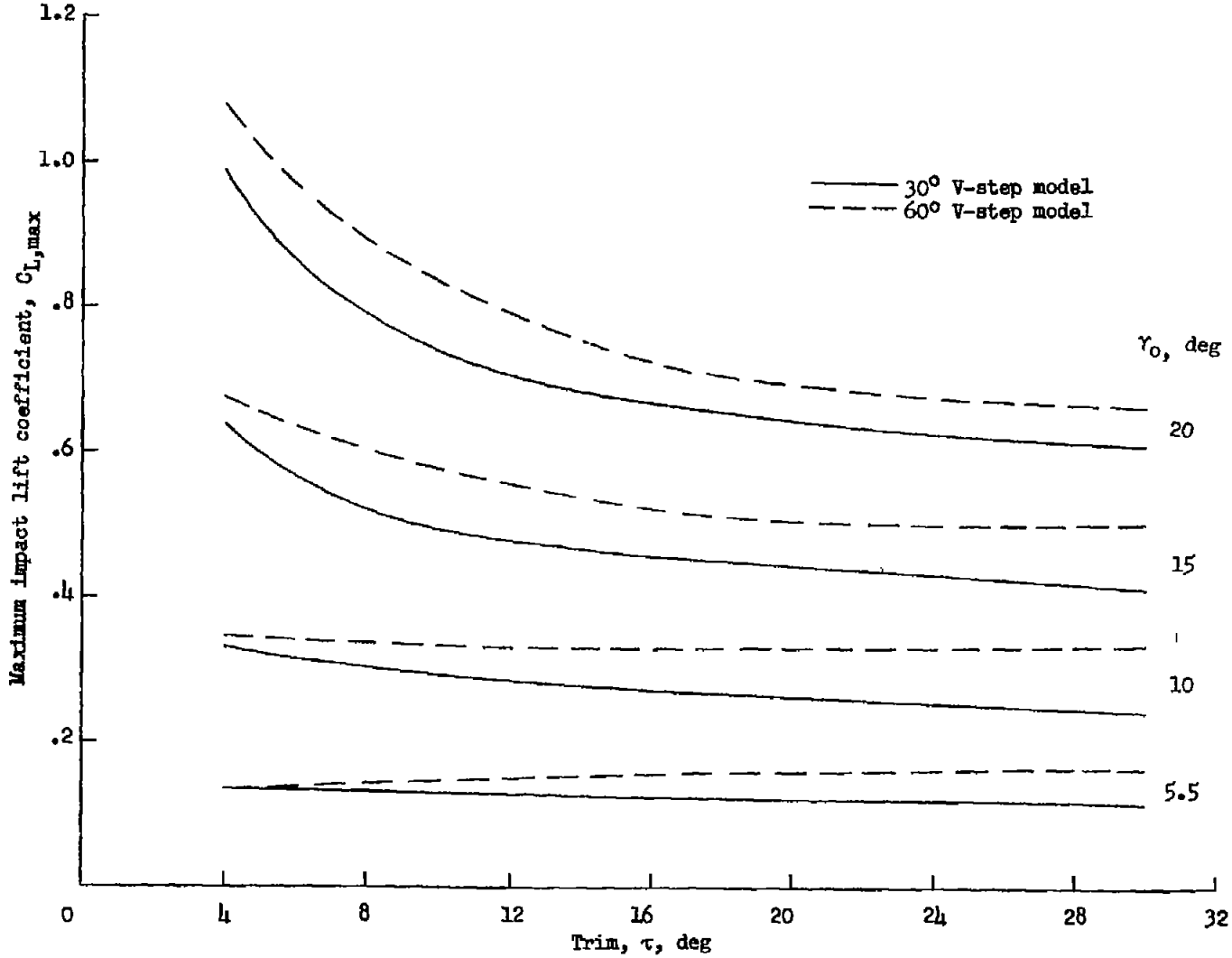

Figure 7.- Variations of faired values of maximum impact lift coefficient with trim angle for 30° and 60° V-step models.

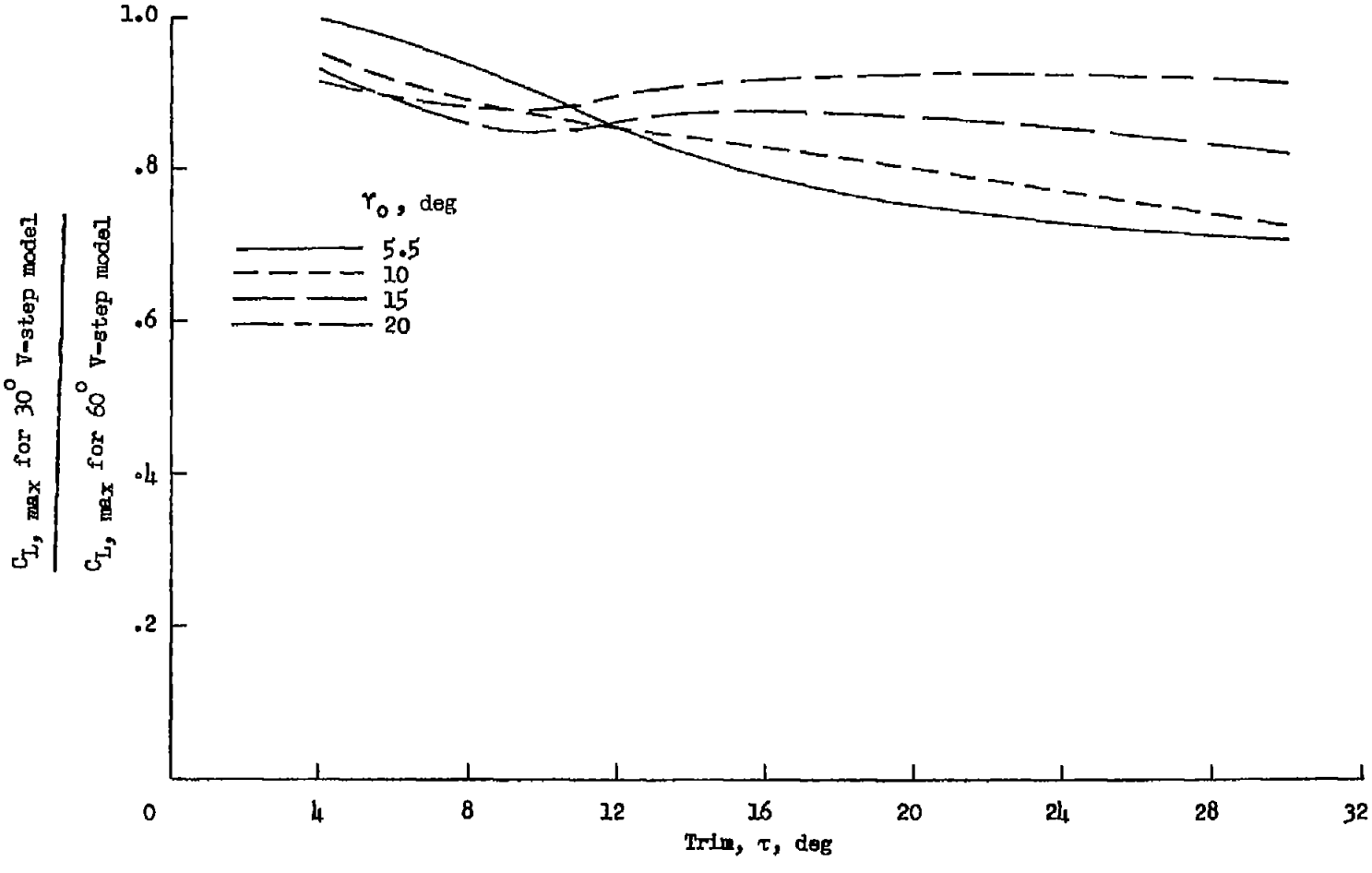

Figure 8.- Variations of ratio of maximum impact lift coefficients for 30° and 60° V-step models with trim angle.

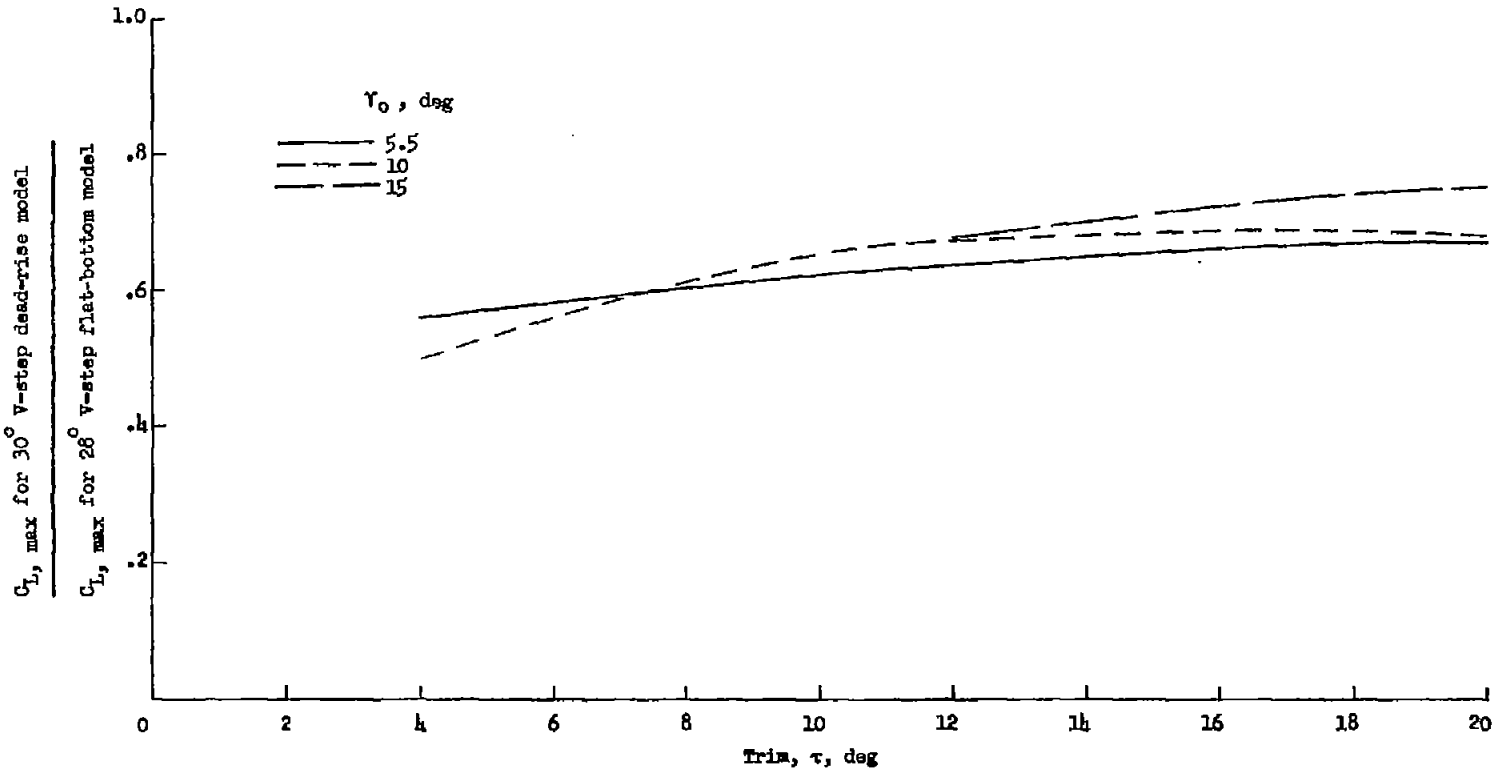

Figure 9.- Variations of ratio of maximum impact lift coefficients for dead-rise and flat-bottom models with V-step plan forms with trim angle.